The interplay of electrostatic and covalent effects in 1-butene oxidation over vanadyl pyrophosphate

D.J. Thompson [a,*], M.O. Fanning [a], B.K. Hodnett [a,b]

[a] *Chemical and Environmental Sciences Department, University of Limerick, CES, Plassey Campus, Limerick, Ireland*
[b] *Materials and Surface Science Institute, University of Limerick, Limerick, Ireland*

Abstract

Quantum mechanical reactivity indices were computed from B3LYP calculations on 1-butene and active site clusters representing stoichiometric and phosphorous-enriched $(VO)_2P_2O_7$ $(1\,0\,0)$ surfaces. Results indicate that 1-butene may chemisorb via formation of a π–cation complex at the stoichiometric (Open) surface, with comparison of local softnesses in 1-butene and the Open active site indicating a strong interaction. Coulombic repulsion at the phosphorous-enriched (Cleft) surface blocks vanadium sites from the C=C region of 1-butene, precluding π–cation complex formation in the Cleft active site. The phosphorous-enriched surface naturally features a greater concentration of nucleophilic terminal P–O oxygen species, which may promote C–H, rather than C–C, bond rupture in subsequent oxidation of adsorbed 1-butene. Hence, a rationale may be offered for both the ease of adsorption, and the low selectivity to maleic anhydride, observed experimentally when 1-butene undergoes oxyfunctionalisation over vanadyl pyrophosphate. Results also indicate that oxidative transformation of *n*-butane over $(VO)_2P_2O_7$ is unlikely to proceed via an olefin intermediate.
© 2003 Elsevier B.V. All rights reserved.

Keywords: Vanadyl pyrophosphate; Quantum chemical calculations; Cluster models; Selective oxidation; Olefin adsorption; Fukui functions; Local softness matching

1. Introduction

The oxyfunctionalisation of *n*-butane over vanadyl pyrophosphate has been the subject of extensive experimental [1–7] and quantum chemical investigation [8–10], due to the unique ability of the catalyst to produce maleic anhydride, a highly-functionalised and hence valuable chemical intermediate, with high selectivity. Studies [2–4,11–13] of butene oxidation over the $(VO)_2P_2O_7$ surface have also appeared, both for its own utility in oxidative transformation to more valuable products and also because butene has been hypothesised as an intermediate in the selective oxidation of *n*-butane to maleic anhydride. Despite the greater reactivity of the olefin substrate, however, *n*-butane remains the feedstock of choice for maleic anhydride synthesis. This is because it has been found that, although $(VO)_2P_2O_7$ is active in butene oxidation, a large fraction of underoxidised C–H cleavage by-products are formed [11,13], decreasing the yield of maleic anhydride. The surface also quickly deactivates, due to strong substrate binding at catalyst active sites [2].

So, the interaction of 1-butene with the vanadyl pyrophosphate surface is investigated in the present study using quantum mechanical reactivity indices, to facilitate comparison between the mode of action

of the $(VO)_2P_2O_7$ surface in catalysing oxidative transformation of the alkane [10] and alkene substrates. Cluster models of both stoichiometric and phosphorous-enriched $(1\,0\,0)$ surfaces are used, called Open [10] and Cleft [10,14] active sites, respectively, with surface-enrichment in phosphorous crucial for selectivity to maleic anhydride in *n*-butane oxidation [14]. Reactivity parameters employed are the same as those used in the *n*-butane oxyfunctionalisation study [10]; electrostatic potential distributions are used to predict favourable orientations of approach of the substrate to the catalyst surface, while absolute electronegativities [15] and local softnesses [15] describe the direction and site-selectivity, respectively, of electron transfer at the substrate–surface interface.

2. Methodology and computational details

Gaussian98 [16] was used for all electronic structure determinations, employing the B3LYP [17] functional in tandem with 6-31G basis sets, and utilising the Natural Population Analysis [18] to compute atomic charges. Restricted and restricted open-shell calculations describe neutral (N_0) and radical cation/anion $(N_0 - 1)/(N_0 + 1)$ systems, respectively. We have previously shown [10] that such model chemistry is sufficient to describe the $(VO)_2P_2O_7$ $(1\,0\,0)$ active site clusters; the electronic properties of 1-butene are also converged at this level of theory.

The concept of local softness [15] unites global and local reactivity descriptors, carrying information on both inherent and site-specific reactivity. Local softness can thus be used to quantify the actual tendency of a molecule to engage in electron transfer interactions, and is calculated by Eq. (1).

$$s(r) = S \times f(r) \tag{1}$$

where s is local softness at point r, S global softness, and f the Fukui function at r.

Application of the finite-difference approximation allows derivation of local softness formulae for both electrophilic and nucleophilic attacks, given in Eq. (2):

$$s^-(r) = S \times f^-(r); \qquad s^+(r) = S \times f^+(r) \tag{2}$$

where '−' and '+' refer to electron-donor and electron-acceptor power, respectively. Local HSAB

theory [15] states that electrostatic interactions maximise net Coulombic attraction at the bimolecular interface while covalent reactions proceed via electron donation from the most basic site(s) in the less electronegative system to the most acidic site(s) in the electron acceptor. Close matching [19] of electron-donor power in the nucleophile with electron-accepting power in the electrophile promotes covalent interaction, with each reaction partner approaching its desired electron configuration.

3. Results and discussion

3.1. Electrostatic potential distributions in 1-butene and $(VO)_2P_2O_7$ $(1\ 0\ 0)$ clusters

$(VO)_2P_2O_7$ $(1\,0\,0)$ clusters feature areas of strong net negative charge over coordinatively-unsaturated terminal P–O oxygens [10], with higher concentration of such species conducive to increased $positive_{substrate} - negative_{surface}$ overlap in electrostatic alignment of the reactant at the catalyst surface, and also selectivity in post-chemisorption steps to maleic anhydride [10]. Shown in Fig. 1 is the molecular electrostatic potential (MEP) surface of 1-butene, followed by an orientation of approach of butene to the Open active site that maximises overlap between substrate hydrogens and surface P–O oxygens while simultaneously placing the strongly-negative C=C region of butene in the vicinity of positive surface vanadium species.

The Cleft cluster, as a model of a phosphorous-enriched, and, by extension (terminal P–O oxygen)-enriched, surface active site, is less likely to feature such an electrostatically-held substrate–surface complex, due to repulsion between C=C carbons and terminal P–O oxygens overhanging vanadium at the pyrophosphate-terminated $(1\,0\,0)$ surface. Hence, butene will preferentially approach surface regions featuring exposed vanadium, i.e. Open, rather than Cleft, active sites.

Once at the surface, any electron transfer will be initiated by donation of electron density from olefinic carbons to vanadium, with concomitant back-donation from vanadium to the carbons, as predicted by absolute electronegativities shown in Table 1 in the next section and local softnesses reported in Section 3.3.

1-Butene MEP distribution

(a)

Electrostatically-held substrate-surface complex

- Terminal P-O oxygen
- Butene C=C region
- Terminal P-O oxygen

● Vanadium   ○ Oxygen
◉ Phosphorous ◉ Carbon
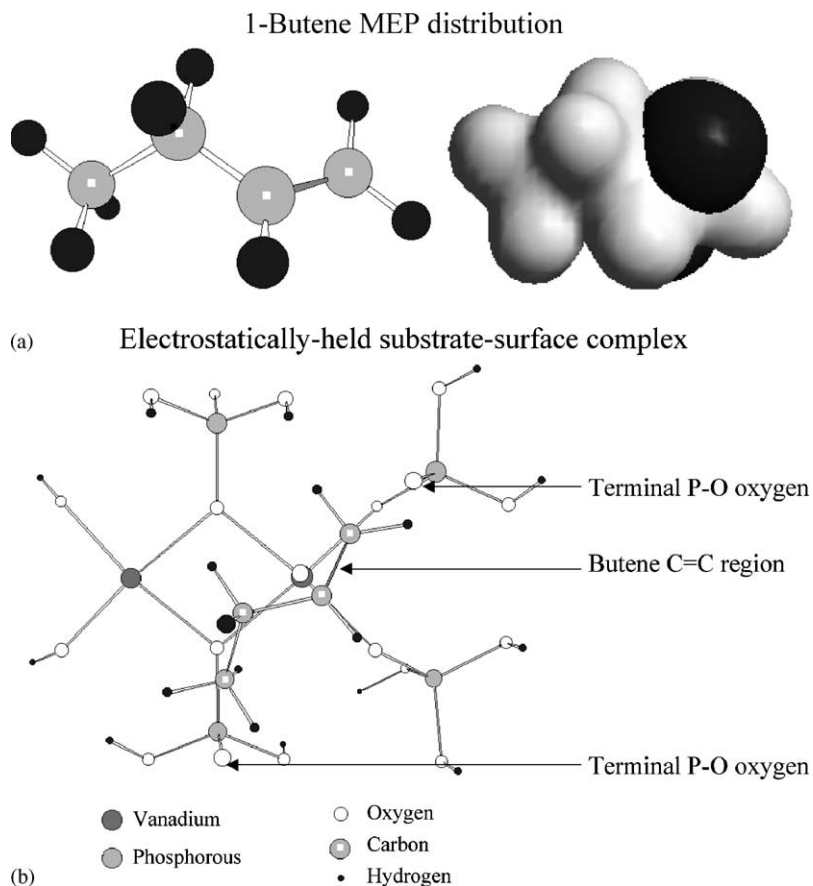(b)   • Hydrogen

Fig. 1. (a) Molecular electrostatic potential (MEP) map for 1-butene. White and black in the MEP surface denotes positive and negative charge, respectively. (b) Electrostatic alignment of 1-butene at the $(VO)_2P_2O_7$ (1 0 0) Open active site cluster.

3.2. Global reactivity in 1-butene and $(VO)_2P_2O_7$ (1 0 0) clusters

Global reactivity indices for 1-butene, along with the Open and Cleft active site clusters, are given in

Table 1
Ionisation potential (I), electron affinity (A), electronegativity (χ), hardness (η), and global softness (S) values

	Global reactive index				
	I	A	χ	η	S
1-Butene	9.51	−3.17	3.17	6.34	0.16
Open active site	5.29	2.31	3.80	1.49	0.67
Cleft active site	6.06	3.54	4.80	1.26	0.79

All values in eV, except S in eV^{-1}. $I = \frac{1}{2}(E_{N_0-1} - E_{N_0})$; $A = \frac{1}{2}(E_{N_0} - E_{N_0+1})$; $\chi = \frac{1}{2}(I + A)$; $\eta = \frac{1}{2}(I - A)$; $S = 1/\eta$.

Table 1. Relative electronegativities dictate that the direction of initial flow of electron density at the substrate–surface interface will be from 1-butene to surface active sites. Global softnesses indicate that the catalyst is generally much more reactive than 1-butene, suggesting low activity for 1-butene chemisorption at $(VO)_2P_2O_7$ (1 0 0) active sites. Of course, observed reactivity depends on both global and local effects.

3.3. Local softnesses in 1-butene and $(VO)_2P_2O_7$ (1 0 0) clusters

Shown in Table 2 below are maximum Fukui functions and associated local softnesses in 1-butene and the catalyst active sites, where local reactivity values refer to sp^2 carbon and vanadium [10] sites in the

Table 2

Comparison of electron donor/acceptor powers in substrate and cluster reaction sites

	Local reactivity index			
	f^-	s^-	f^+	s^+
1-Butene	0.36	0.06	0.30	0.05
n-Butane ($S = 0.12$)	0.07	0.01	0.14	0.02
Open active site	0.17	0.11	0.13	0.09
Cleft active site	0.24	0.19	0.14	0.11

$f^- = (q_{N_0-1} - q_{N_0})$; $s^- = S \times f^-$; $f^+ = (q_{N_0} - q_{N_0+1})$; $s^+ = S \times f^+$.

substrate and clusters, respectively. Included also are analogous values for n-butane, to allow comparison of substrate-catalyst reaction site matching for olefin and paraffin substrates.

In contrast to electron transfer between n-butane and catalyst active sites [10], vanadium accepts electron density from, and donates electron density to, the same atoms in 1-butene, leading to formation of an alkene-metal complex described by the Dewar–Chatt–Duncanson model [20]; donation of electron density from the C=C π orbital is accompanied by backbonding into the empty π^* orbital on the olefin.

Inspection of local softness values in Table 2 indicates that the softness of surface vanadium species for nucleophilic attack (filling of low-lying empty d-levels [10]) by sp^2 carbon is approximately twice the susceptibility of the olefinic carbon to electrophilic attack; hence, forward-donation from both sp^2 carbons to vanadium leads to close matching of electron donor sites in the substrate with surface acid sites. Similarly, electrophilicity due to the olefin π^* bond is similar in magnitude to surface basicity manifested through *occupied* vanadium d-levels.

1-Butene and n-butane have similarly low global softnesses, suggesting an almost equally low degree of electron transfer [15] when either n-butane or 1-butene interact with the highly reactive (VO)$_2$P$_2$O$_7$ (1 0 0) surface. The more localised reaction sites in 1-butene however, lead to significantly higher local softnesses in 1-butene as shown in Table 2. This indicates that 1-butene will react more strongly than n-butane with the (VO)$_2$P$_2$O$_7$ (1 0 0) surface, on the basis of closer matching [19] of the substrate and surface electron transfer sites in terms of local HSAB theory [15].

In summary, 1-butene forms a π-complex with vanadium, as hypothesised from experimental stud-

ies [12]. Close matching of local softnesses at the substrate–surface interface may explain why 1-butene interacts much more strongly than n-butane with the vanadyl pyrophosphate surface [2,4], at lower temperatures and with higher rates of adsorption.

3.4. (VO)$_2$P$_2$O$_7$ (1 0 0) as catalyst for 1-butene mild oxidation

Our results show that 1-butene can chemisorb strongly at the Open (VO)$_2$P$_2$O$_7$ (1 0 0) surface. The availability of nucleophilic terminal P–O oxygen species [10] for subsequent controlled oxidation of adsorbed 1-butene, though, is very limited at this stoichiometric surface, which may explain why 1-butene oxidation over vanadyl pyrophosphate typically yields a high proportion of underoxidised C–H cleavage products [11,13], since π-complex formation necessitates substrate interaction with areas of exposed surface vanadium, that is, the Open (terminal P–O oxygen deficient) active site configuration.

Two features of the vanadyl pyrophosphate (1 0 0) surface suggest reasons why vanadyl phosphate (VOPO$_4$) is a better [12] catalyst for 1-butene selective oxidation to maleic anhydride. The first relates to the strength of the sorption interaction, while the second is concerned with the accessibility of surface vanadium sites to butene.

Firstly, the V^V ion in VOPO$_4$ is formally d^0, compared to V^{IV} (d^1) in (VO)$_2$P$_2$O$_7$, which implies formation of a more weakly-bound complex (due to decreased surface backbonding), and hence longer times to catalyst deactivation.

Secondly, the C=C region of 1-butene has a repulsive Coulombic interaction with the phosphorous-enriched vanadyl pyrophosphate active site, as explained in Section 3.1. It has been noted previously [2] that excess phosphorous in the precursor to (VO)$_2$P$_2$O$_7$, leading naturally to excess phosphorous at the active surface [4], helps to keep vanadium in an oxidation state of 4+, making VOPO$_4$ unlikely to feature surface-enrichment in phosphorous. Hence, a high concentration of VOPO$_4$ surface vanadium sites will be available for 1-butene chemisorption.

Further experimental investigations on the effect of surface P:V ratio in 1-butene oxidation over (VO)$_2$P$_2$O$_7$ and VOPO$_4$ catalysts, and also ab initio modelling of the vanadyl phosphate active surface, are

necessary for a deeper understanding of 1-butene oxy-functionalisation over VPO catalysts. However, the very different modes of action calculated for *n*-butane [10] and 1-butene interaction with the $(VO)_2P_2O_7$ (1 0 0) surface indicate that butene may not be an intermediate in *n*-butane oxidation to maleic anhydride over vanadyl pyrophosphate.

References

[1] M.A. Pepera, J.L. Callahan, M.J. Desmond, E.C. Milberger, P.R. Blum, N.J. Bremer, J. Am. Chem. Soc. 107 (1985) 4883.

[2] G. Centi, F. Trifiro, J.R. Ebner, V.M. Franchetti, Chem. Rev. 88 (1988) 55.

[3] G. Centi, Catal. Today 16 (1993) 1.

[4] F. Cavani, F. Trifiro, Chemtech 24 (1994) 18.

[5] P.L. Gai, Top. Catal. 8 (1999) 97.

[6] J.C. Volta, C. R. Acad. Sci., Ser. IIC: Chim. 3 (2000) 717.

[7] B.K. Hodnett, Heterogeneous Catalytic Oxidation: Fundamental and Technological Aspects of the Selective and Total Oxidation of Organic Compounds, Wiley, New York, 2000.

[8] M. Witko, R. Tokarz, J. Haber, K. Hermann, J. Mol. Catal. A: Chem. 166 (2001) 59.

[9] A. Haras, H.A. Duarte, D.R. Salahub, M. Witko, Surf. Sci. 513 (2001) 367.

[10] D.J. Thompson, M.O. Fanning, B.K. Hodnett, J. Mol. Catal. A: Chem. 198 (2003) 125.

[11] J. Ziolkowski, E. Bordes, P. Courtine, J. Catal. 122 (1990) 126.

[12] E. Bordes, C. R. Acad. Sci., Ser. IIC: Chim. 3 (2000) 725.

[13] V.V. Guliants, S.A. Holmes, J. Mol. Catal. A: Chem. 175 (2001) 227.

[14] J.R. Ebner, M.R. Thompson, Catal. Today 16 (1993) 51.

[15] R.G. Parr, W. Yang, Density-Functional Theory of Atoms and Molecules, Oxford University Press, Oxford, 1989.

[16] M.J. Frisch, G.W. Trucks, H.B. Schlegel, G.E. Scuseria, M.A. Robb, J.R. Cheeseman, V.G. Zakrzewski, J.A. Montgomery Jr., R.E. Stratmann, J.C. Burant, S. Dapprich, J.M. Millam, A.D. Daniels, K.N. Kudin, M.C. Strain, O. Farkas, J. Tomasi, V. Barone, M. Cossi, R. Cammi, B. Mennucci, C. Pomelli, C. Adamo, S. Clifford, J. Ochterski, G.A. Petersson, P.Y. Ayala, Q. Cui, K. Morokuma, D.K. Malick, A.D. Rabuck, K. Raghavachari, J.B. Foresman, J. Cioslowski, J.V. Ortiz, A.G. Baboul, B.B. Stefanov, G. Liu, A. Liashenko, P. Piskorz, I. Komaromi, R. Gomperts, R.L. Martin, D.J. Fox, T. Keith, M.A. Al-Laham, C.Y. Peng, A. Nanayakkara, M. Challacombe, P.M. W. Gill, B. Johnson, W. Chen, M.W. Wong, J.L. Andres, C. Gonzalez, M. Head-Gordon, E.S. Replogle, J.A. Pople, Gaussian98, Revision A.8, Gaussian Inc., Pittsburgh, PA, 1998.

[17] A.D. Becke, J. Chem. Phys. 98 (1993) 5648.

[18] A.E. Reed, R.B. Weinstock, F. Weinhold, J. Chem. Phys. 83 (1985) 735.

[19] J.L. Gazquez, F. Mendez, J. Phys. Chem. 98 (1994) 4591.

[20] M.J.S. Dewar, The Molecular Orbital Theory of Organic Chemistry, McGraw-Hill, Maidenhead, NY, 1969.